DEM-SJM combined 2D-hydraulic fracturing simulation for consideration of the influence of differential stress

Hayate OHTANI[1], Hitoshi MIKADA[1] and Junichi TAKEKAWA[1]
[1]Dept. of Civil and Earth Res. Eng., Kyoto University

For improving the production of conventional oil and shale gas, the practice of hydraulic fracturing has been increasing in recent years. In addition, hydraulic fracturing is used for the development of geothermal energy known as hot dry rock (HDR) geothermal power, and enhanced geothermal system (EGS), and for measuring the rock failure strength and the orientation of principal stress direction, etc. On the other hand, hydraulic fracturing has some environmental impact, such as pollution caused by chemical substances in injected proppant or fluid, induced seismicity, etc. Since it is necessary to minimize the environmental impact, techniques to predict propagating directions and distances of fractures to be generated hydraulically, which are known still very difficult, have been waited for. In this paper, we demonstrate the influence of differential stress and the anisotropy using numerical experiments based on distinct element method (DEM) combined with smooth joint model (SJM). Hydraulic fractures in general propagate in the direction of maximum principal stress on large differential stress conditions. As the differential stress decreased, the propagating directions hydraulic fractures curves to the direction of bedding plane, i.e., anisotropic direction of weak rock strength, and sometimes fractures branch to plural directions. These results suggest that the behavior and propagating direction of hydraulic fractures are strongly influenced by both the differential stress and the rock strength anisotropy in the underground shallow layer.

1. INTRODUCTION

By the development of hydraulic fracturing techniques, the amount of production of hydrocarbon (oil/shale gas) has greatly increased. This technique is also used for hot dry rock (HDR) geothermal power, enhanced geothermal system (EGS), measuring the rock failure strength and the orientation of principal stress direction.

To maximize the productivity, long and complicated fracture networks need to be created. On the other hand, exuding injected fluid from these fractures could contaminate the aquifer near the reservoir. Therefore, prediction and monitoring of the behavior of hydraulically induced fractures is indispensable. However, there are many factors which can influence on the behavior of hydraulically induced fractures, i.e. viscosity of the injected fluid[1)], in-stress[2)], background stress field[3)], and strength heterogeneity of host rock [4)].

It's well-known that physical and mechanical properties of shale rock show anisotropy, and existence of the bedding planes affects the pattern of macroscopic failure in uniaxial compression tests and Brazilian tests[5)].

Now, hydraulic fracturing is assumed to be conducted in the underground shallow layer where a lot of types of differential stress are expected, and our previous study showed that the combination effect of in-situ stress state and strength anisotropy of shale rock should be considered for predicting the behavior and propagating direction of hydraulically induced fractures. Although the numerical experimental results indicated the importance of taking strength anisotropy into consideration, the representation of strength anisotropy is not sufficient. In the present study, we newly introduce smooth joint model (SJM) into the hydraulic fracturing simulation for more accurate numerical experiments. At first, we examine the reproducibility of strength anisotropy using uniaxial compressive tests. Next, we apply the developed method to hydraulic fracturing simulation with various differential stresses. Finally, we discuss the relationship between the magnitude of differential stress and direction of hydraulic fractures.

2. METHOD

(1) Distinct element method

For the simulation, DEM (Distinct Element Method) is used since it can represent complicated behavior and failure of rocks[6)]. In DEM, a target is represented as a mass of small particles imaginarily bonded with each other. When there is a bond between particles, attraction and repulsion could act on the particles, and when there isn't, only repulsion

could act on the particles. The bonds have normal and shear strength. When normal or shear stress which acts on the bond exceeds the strength, it will break, and the two particles never be bonded. Breaking bond means that one small crack is generated. By following the movement of particles and breaking bonds, the behavior of the whole continuum can be considered.

(2) Fluid flow algorithm

In hydraulic fracturing simulation, we need to consider not only the behavior of particles; grain part, but also the behavior of fluid; fluid part. In order to follow the behavior of injected fluid, fluid flow algorithm[7),1)] (FFA) is used. In FFA, there are mainly 3 rules.

1. Imaginary pores are supposed to exist at the center of the enclosed domain by particles, and they are connected to each other by flow channels.
2. Depending on the difference of pore pressures, the amount of fluid which moves from one pore to another one will be determined using the concept of Hagen-Poiseuille flow.
3. On the particles, two kinds of force will act; the force by pore pressure and the force by the fluid flow in the flow channel.

Aperture of a flow channel 'w' changes as the normal stress F at the contact point changes, and is described as

$$w = \frac{w_0 F_0}{F + F_0} \tag{1}$$

where w_0 is assumed initial aperture set between particles just touching, and F_0 is the normal stress at which the aperture decreases to half of its initial aperture.

(3) Representation of anisotropy

In the procedure of representing anisotropy, two methods are combined to DEM-SJM combined method. First one is our original method[8)] and another is SJM[9)]. In the first method, the macroscopic empirical equation for uniaxial tensile strength of granite[10)] is applied to microscopic DEM-parameters. This method enables us to represent anisotropy to some extent.

Bonds' tensile strength σ is given as

$$\sigma = \sigma_{max} cos^2(\phi - \theta) + \sigma_{min} sin^2(\phi - \theta) \tag{2}$$

and bonds' shear strength τ is given as

$$\tau = \tau_{max} cos^2(\phi - \theta) + \tau_{min} sin^2(\phi - \theta) \tag{3}$$

where σ_{max} , τ_{max} and σ_{min} , τ_{min} are the maximum and the minimum values of bond's tensile and shear strength, respectively. ϕ is the bond's angle, and θ is the anisotropy angle shown in Figure 1.

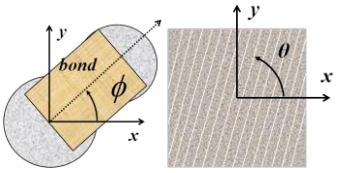

Figure 1 The definition of ϕ and θ

Young modulus of the whole continuum E_θ is obtained using the compliance matrix, and given as

$$E_\theta = \frac{E_0 E_{90}}{E_0 sin^2\theta + E_{90} cos^2\theta} \tag{4}$$

where E_0 is the Young modulus when bedding plane is perpendicular to the loading axis, and E_{90} is the Young modulus when bedding plane is parallel to the loading axis. The loading axis corresponds with y-axis in Figure 1. This macroscopic theoretical relation is applied to the microscopic parameter E, and given as

$$E = \frac{E_{max} E_{min}}{E_{max} sin^2(\phi - \theta) + E_{min} cos^2(\phi - \theta)} \tag{5}$$

In the conventional DEM, if an arbitrary particle moves in arbitrary direction, it should rebound when there are other particles ahead. Moreover, the orientations of the initial local particle contacts could cause inherent roughness problems. By introducing SJM, however, these problems are eliminated, and the moving direction of particles could be controlled. In SJM, there are smooth joint planes, and a part of a particle is ignored as shown in Figure 2.

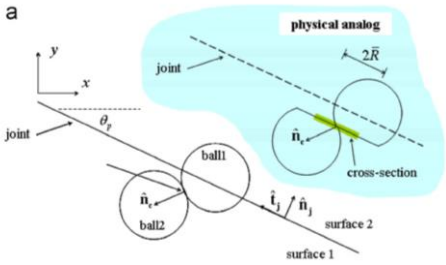

Figure 2 The concept of SJM[9)]

When the following condition is fulfilled, SJM is introduced; the line segment which connects a center of a particle and a center of a particle adjacent to the particle intersects with a smooth joint plane. Then the strength of the bond between the particles is set to the minimum value. This makes it easier to generate a microcrack or a fracture in the direction of a smooth joint plane; a weak plane or a bedding plane.

(4) Calibration

We tuned microscopic parameters of DEM by using ten realizations. In tuning, uniaxial compression test (UCT), uniaxial tension test (UTT), and permeability test are conducted. Only the result of uniaxial compression test is shown in Figure 3. The numerical result of uniaxial compression test[8] and the experimental result of uniaxial compression test[5] are shown in Figures 4 and 5, respectively. The vertical axis of these figures is the uniaxial compressive strength (UCS).

We can see that the result has greatly improved. In Ohtani et al. (2017)[8], the shape of the result was U-curved one, and become minimum when anisotropy angle is equal to 45 deg. On the other hand, the shape of the result in Cho et al. (2012) was U-curved one, and become minimum when anisotropy angle is equal to 60 deg. In this time, the problem has solved by introducing SJM.

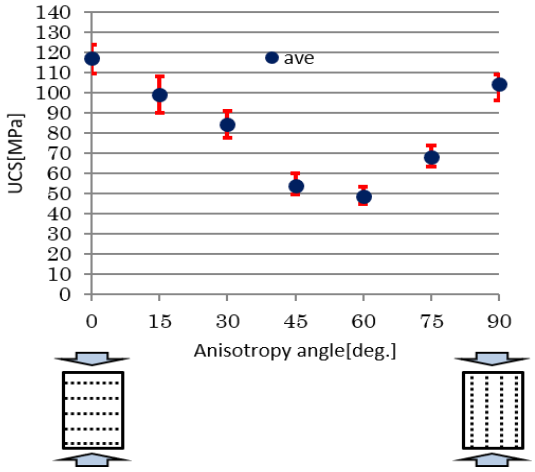

Figure 3 The result of UCT

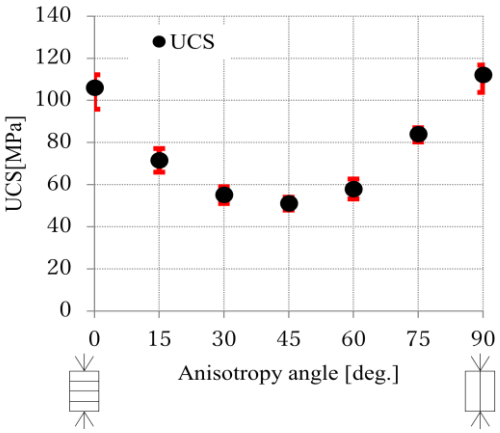

Figure 4 The result of UCT[8]

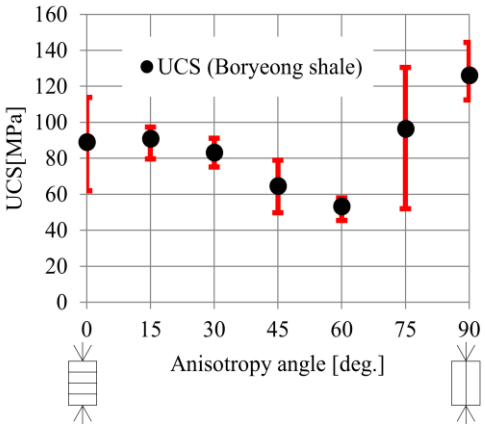

Figure 5 The result of UCT[5]

3. SIMULATION MODEL

Hydraulic fracturing simulation model is shown in Figure 6(a) and 6(b). The bedding plane is assumed parallel to the ground surface since this research focuses on hydraulic fracturing in horizontally drilled borehole. Model size is 1.2m in both width and height, and a borehole whose diameter is 0.1m is set at the center of the model. The simulations are demonstrated on different differential stresses. Vertical direction is defined as 'z-direction', and horizontal direction as 'y-direction'. The distance between bedding planes which is colored black in Figure 6(b) is 0.2 m. Through the borehole, fracturing fluid is injected. Degree of initial saturation of all pores is 60.0 %, porosity of the model is 4.0 %, bulk modulus of fluid is 2.0 GPa, viscosity of fluid is 0.1×10^{-3} Pa·m, and flow rate is 3.0×10^{-3} m^2/s. We prepared totally 11 models from pattern 1 (P1) to pattern 11 (P11). In all models, σ_z is 10 MPa. In P1, σ_z is 10 MPa and σ_y is 5.0 MPa. In other models, σ_y increases with an interval of 0.5

MPa. In P4, for example, σ_y is 6.5 MPa, and σ_y is 8.5 MPa in P8, and σ_y is 10 MPa in P11.

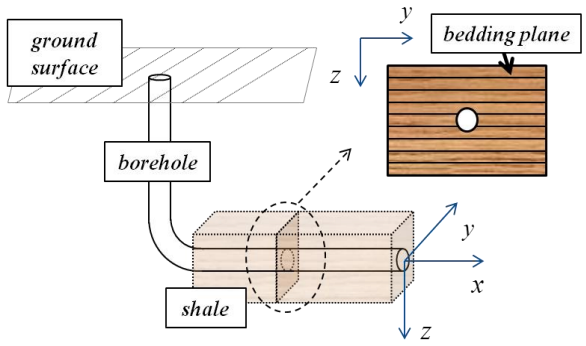

Figure 6(a) Hydraulic fracturing in horizontally drilled borehole[11)]

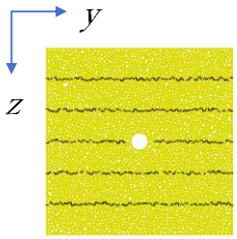

Figure 6(b) Simulation model

4. RESULTS

Pressure changes in borehole of each model are presented in Figure 7, and simulation results are presented in Figure 8. Breaking bonds are expressed as colored bars, and the saturated and unsaturated areas as blue domains with gradation. A red bar means a bond break in tension where SJM is not introduced. A black bar means a bond break in shear where SJM is not introduced. A Pink bar means a bond break in tension where SJM is introduced. A Green bar means a bond shear break in tension where SJM is introduced. A yellow bar is a bond shear break in compression where SJM is introduced.

The results are roughly divided into three types. First one 'type-a' is that hydraulically induced fractures propagated in the direction of maximum principal stress. Second one 'type-b' is that hydraulically induced fractures propagated neither in the direction of maximum principal stress nor in the direction of weak plane or bedding plane. Third one 'type-c' is that hydraulically induced fractures propagated in the direction of weak plane of bedding plane. The results of P1 and P2 belong to 'type-a', those of P3, P4, P5, P6, P7, P8 and P9 belong to 'type-b', and those of P10, P11 belong to 'type-c'. In P5, a blanched fracture was created.

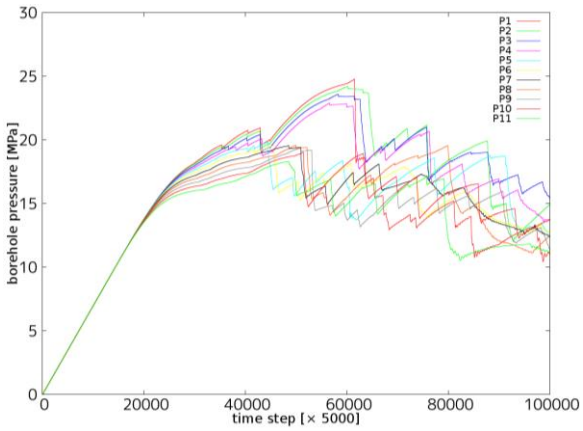

Figure 7 Pressure changes in borehole

5. DISCUSSION

As mentioned above, the results are roughly divided into three types according to the direction in which hydraulically induced fractures propagated.

type-a: The direction of maximum principal stress

type-b: The direction of neither maximum principal stress nor weak plane or bedding plane

type-c: The direction of weak plane of bedding plane

In isotropic media, hydraulically induced fractures are usually expected to propagate in the direction of maximum principal stress. However, in anisotropic media, that could be affected by anisotropy and differential stress. Figure 8 also indicates that in anisotropic media the smaller differential stress becomes, the more directions of hydraulically induced fractures are influenced by anisotropy.

Wang et al. (2017)[12)] showed that even when the fracture intersects with the bedding plane at right angle, it could propagate in the direction of bedding plane and blanch from the intersection point. The result of P5 is in good agreement with this example as shown in Figures 9 and 10. The reason why these branched fractures were generated hasn't revealed yet, and we would like to investigate the reason in our future study.

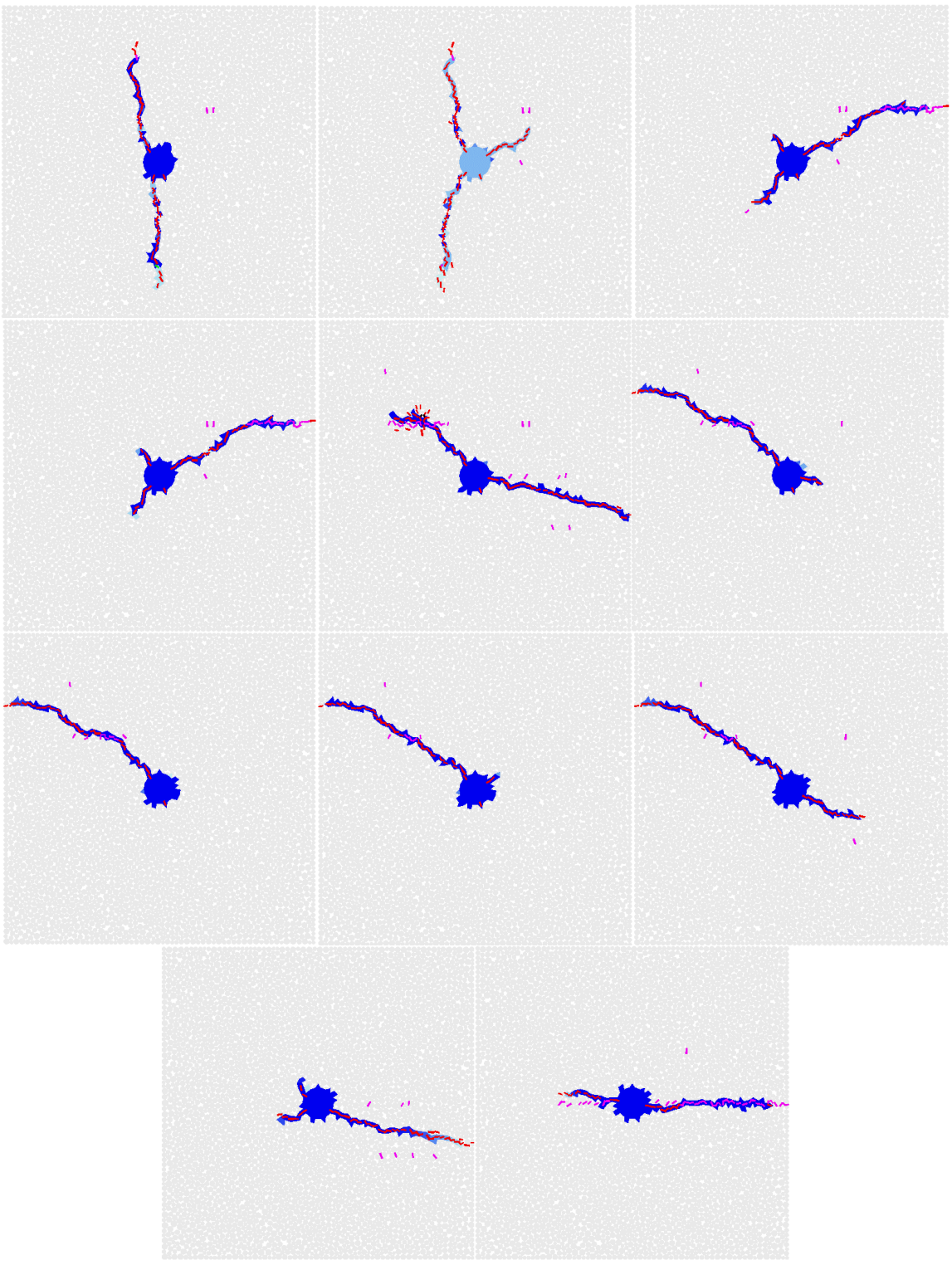

Figure 8 The result of simulations

The pictures in the top section are the results in P1, P2, P3 from the left side. The pictures in the 2nd section are the results in P4, P5, P6from the left side. The pictures in the 3rd section are the results in P7, P8, P9from the left side. The pictures in the 4th section are the results in P10, P11from the left side.

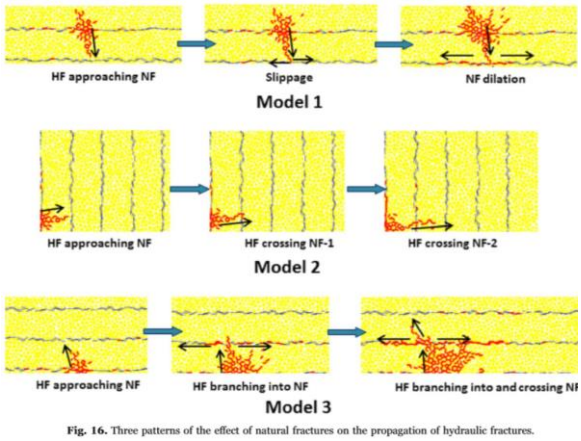

Fig. 16. Three patterns of the effect of natural fractures on the propagation of hydraulic fractures.

Figure 9 The result of Wang et al.,2017

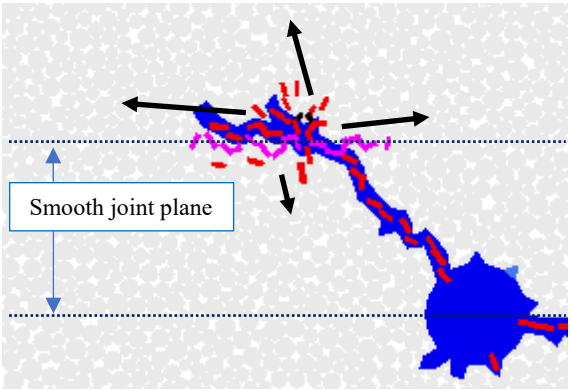

Figure 10 The result of P5

6. CONCLUSION

In order to investigate how differential stress could influence on hydraulic fracturing in rocks with mechanical anisotropy, numerical experiments based on DEM have been conducted. The results give us the following conclusions. According to the difference of the differential stress, propagating directions of hydraulically induced fracture can be roughly divided into three types.

Type-a: The direction of maximum principal stress

Type-b: The direction of neither maximum principal stress nor weak plane or bedding plane

Type-c: The direction of weak plane or bedding plane.

These results indicate that in anisotropic media the smaller differential stress becomes, the more directions of hydraulically induced fractures are influenced by anisotropy, i.e. the fractures do not always propagate in the direction of bedding plane or maximum principal stress. Moreover, the fracture plane could make branches when the induced fracture reaches a weak bedding plane.

REFERENCES

1) Shimizu, H., Murata, S. and Ishida, T., 2011., The distinct element analysis for hydraulic fracturing in hard rock considering fluid viscosity and particle size distribution, *International Journal of Rock & Mining sciences*, **48**, 712-727.
2) Nasehi, M. J. and Mortazavi, A., 2013., Effects of in-situ stress regime and intact rock strength parameters on the hydraulic fracturing, *Journal of Petroleum Science and Engineering*, **108**, 211–221.
3) Okubo, K., Mikada, H., Goto, T. and Takekawa, J., 2013., Stress distribution in fractured medium and fracture propagation due to formation pressure changes, *SEG Technical Program Expanded Abstracts 2013*, 626-630.
4) Nagaso, M., Mikada, H. and Takekawa, J., 2016., Mechanism of complex fracture creation in hydraulic fracturing, *The 20th International Symposium on Recent Advances in Exploration Geophysics (RAEG 2016).*
5) Cho, J.W., Kim, H., Jeon, S. and Min, K.B., 2012., Deformation and strength anisotropy of Asan gneiss, Boryeong shale, and Yeoncheon schist, *International Journal of Rock & Mining sciences*, **50**, 158-169.
6) Potyondy, D.O. and Cundall, P.A., 2004., A bonded-particle model for rock, *International Journal of Rock & Mining sciences*, **41**, 1329-1364.
7) Al-Busaidi, A., Hazzard, J.F. and Young, R.P., 2005., Distinct element modeling of hydraulically fractured Lac du Bonnet granite, *Journal of Geophysical Research*, **110**.
8) Ohtani, H., Mikada, H. and Takekawa, J., 2017., Fundamental research on the role of differential stress in hydraulic fracturing in strength-anisotropic medium, *The 21st International Symposium on Recent Advances in Exploration Geophysics (RAEG 2017).*
9) Ivars, D.M., Pierce, M.E., Darcel, C., Reyes-Montes, J., Potyondy, D.O., Young, R.P. and Cundall, P.A., 2011., The synthetic rock mass approach for jointed rock mass modeling, *International Journal of rock mechanics & Mining Sciences*, **48**, 219-244.
10) Kosugi, M. and Kobayashi H.,1986, *Suiatsuhasaikikou ni okeru ouryokujyotai, kousei no keisha oyobi kizonkiretsu no eikyo –ihouseiganseki ni okeru suiatsuhasai ni kansuru zikkentekikenkyu (dai2hou)-*, *Journal of the Mining and Metallurgical Institute of Japan,* **102**, 567-573 (in JAPANESE).
11) Ohtani, H., Mikada, H. and Takekawa, J., 2017., Hydraulic fracturing simulation in different differential stresses and anisotropic media, *SEG Technical Program Expanded Abstracts 2017*, 3776-3780.
12) Wang, T., Hu, w., Elsworth, D., Zhou, W., Zhou, W., Zhao, X. and Zhao, L., 2017., The effect of natural fractures on hydraulic propagation in coal seams, *Journal of Petroleum Science and Engineering*, **150**, 180-190.